

• Supplementary File •

Transmission Success Probability Analysis of Vehicle Users With Mobile Relays Under Mobility Models

Di WU¹ & Sheng HUANG^{2*}

¹College of Pharmacy and Biological Engineering, Chengdu University, Chengdu 610106, China;

²No.10 Institute of China Electronic Technology Corporation, ChengDu 610036, China

Appendix A Proof of Proposition 1

The transmission success probability of the backhaul link (B ↔ R) can be derived by

$$\begin{aligned} \Pr(\text{SINR}_{\text{B,R}}(d) \geq \beta_{\text{B,R}}) &= E_I \left[\Pr \left(\frac{\sum_{l=1}^L P_B d^{-\alpha} X_{\text{B,R}}^l}{I + N_0} \geq \beta_{\text{B,R}} \right) \right] \\ &\stackrel{(a)}{=} E_I \left[Q \left(L m_B, \frac{m_B \beta_{\text{B,R}} (I + N_0)}{P_B d^{-\alpha}} \right) \right] \\ &\stackrel{(b)}{=} \sum_{n=0}^{L m_B - 1} \frac{(-1)^n}{n!} \frac{\partial^n}{\partial s^n} \left[\mathcal{L}_{\mathbf{N}}(s) \mathcal{L}_{\mathbf{Y}}(s) \right]_{s=1}, \end{aligned} \quad (\text{A1})$$

where $\mathbf{N} = \frac{m_B \beta_{\text{B,R}} N_0}{P_B d^{-\alpha}}$ and $\mathbf{Y} = \frac{m_B \beta_{\text{B,R}} I}{P_B d^{-\alpha}}$. Specifically, (a) follows the probability density function of $X_{\text{B,R}}^l$ and $Q(a, z)$ is the regularized upper incomplete Gamma function [1]. (b) is derived by applying $Q(a, z) = \sum_{n=0}^{a-1} z^n e^{-z} / n!$ for a positive integer a [2].

Then, the Laplace transform $\mathcal{L}_{\mathbf{N}}(s) = \exp(-\frac{s m_B \beta_{\text{B,R}} N_0}{P_B d^{-\alpha}})$ and the Laplace transform $\mathcal{L}_{\mathbf{Y}}(s)$ is given by

$$\begin{aligned} \mathcal{L}_{\mathbf{Y}}(s) &= E_I \left[\exp \left(-s m_B \beta_{\text{B,R}} d^\alpha I P_B^{-1} \right) \right] \\ &\stackrel{(c)}{=} \prod_{k=1}^K \prod_{y \in \Phi_k} E_{I_{k,y,R}} \left[\exp \left(-\frac{s m_B \beta_{\text{B,R}} P_k X_{k,y,R}}{P_B d^{-\alpha} \|y\|^\alpha} \right) \right] \\ &\stackrel{(d)}{=} \exp \left(-\sum_{k=1}^K \pi \lambda_k d^2 \left(\frac{s m_B \beta_{\text{B,R}} P_k}{P_B} \right)^{\frac{2}{\alpha}} \times \Gamma \left(1 - \frac{2}{\alpha} \right) E \left[X_{k,y,R}^{\frac{2}{\alpha}} \right] \right), \end{aligned} \quad (\text{A2})$$

where (c) follows the independence of $I_{k,y,u}$ and (d) follows [3, eq. (3.20)] by using the probability generating functional. Applying $E \left[X_{k,y,R}^{\frac{2}{\alpha}} \right] = m_I^{-\frac{2}{\alpha}} \Gamma(\frac{2}{\alpha} + m_I) / \Gamma(m_I)$ [2], $\mathcal{P}_{\text{B,R}}(\mathcal{R}_{\text{th}}, d)$ is then obtained. Likewise, $\mathcal{P}_{\text{B,V}}(\mathcal{R}_{\text{th}}, d)$ and $\mathcal{P}_{\text{R,V}}(\mathcal{R}_{\text{th}})$ are proved similarly.

Appendix B Proof of Proposition 2

Letting $\lambda_k \rightarrow 0$ in $\mathcal{P}_{\text{B,V}}(\mathcal{R}_{\text{th}}, d)$ gives

$$\mathcal{P}_{\text{DS}}^N(\mathcal{R}_{\text{th}}, d) = \sum_{n=0}^{m_B - 1} \frac{\left(\frac{m_B \beta_{\text{B,V}} N_0}{P_B d^{-\alpha} \xi} \right)^n}{n!} \exp \left(-\frac{m_B \beta_{\text{B,V}} N_0}{P_B d^{-\alpha} \xi} \right). \quad (\text{B1})$$

Then, the ergodic transmission success probability of the *direct* strategy in the noise-limited regime under the RW model is given by

$$\mathcal{P}_{\text{DS}}^{\text{RW}}(\mathcal{R}_{\text{th}}) = \int_0^D \sum_{n=0}^{m_B - 1} \frac{1}{n!} \left(\frac{\beta_{\text{B,V}} \kappa d^\alpha}{\xi} \right)^n \exp \left(-\frac{\beta_{\text{B,V}} \kappa d^\alpha}{\xi} \right) f_{\text{D}}^{\text{RW}}(d) dd$$

* Corresponding author (email: huangshengcetc10@163.com)

$$\begin{aligned}
 &= \sum_{n=0}^{m_B-1} \frac{(\beta_{B,V}\kappa)^n}{\xi^n n!} \int_0^D d^{m\alpha} \exp\left(-\frac{\beta_{B,V}\kappa d^\alpha}{\xi}\right) \frac{2d}{D^2} dd \\
 &\stackrel{t=\frac{\beta_{B,V}\kappa}{d^{-\alpha}\xi}}{=} \sum_{n=0}^{m_B-1} \frac{2}{n! D^2} \left(\frac{\xi}{\beta_{B,V}\kappa}\right)^{\frac{2}{\alpha}} \int_0^{\frac{\beta_{B,V}\kappa}{D^{-\alpha}\xi}} t^{n+\frac{2}{\alpha}-1} \exp(-t) dt.
 \end{aligned} \tag{B2}$$

Then, $\mathcal{P}_{DS}^{RW}(\mathcal{R}_{th})$ is obtained using the lower incomplete Gamma function $\gamma(a, z) \triangleq \int_0^z t^{a-1} e^{-t} dt$ [1]. Likewise, $\mathcal{P}_{RS}^{RW}(\mathcal{R}_{th})$, $\mathcal{P}_{DS}^{RWP}(\mathcal{R}_{th})$, and $\mathcal{P}_{RS}^{RWP}(\mathcal{R}_{th})$ are proved similarly.

Appendix C Proof of Proposition 3

By letting $\frac{P_B d^{-\alpha}}{N_0} \rightarrow \infty$ in $\mathcal{P}_{B,V}(\mathcal{R}_{th}, d)$, the ergodic transmission success probability of the *direct* strategy in the interference-limited regime under the RW model is given by

$$\begin{aligned}
 \mathcal{P}_{DS}^{RW}(\mathcal{R}_{th}) &= \int_0^D \mathcal{P}_{DS}^I(\mathcal{R}_{th}, d) \cdot f_D^{RW}(d) dd \\
 &\stackrel{(e)}{=} \sum_{n=0}^{m_B-1} \frac{(-1)^n}{n!} \frac{\partial^n}{\partial s^n} \left[\int_0^D \exp\left(-d^2 \sum_{k=1}^K \pi \psi_k s^{\frac{2}{\alpha}} \left(\frac{\beta_{B,V} m_B}{P_B}\right)^{\frac{2}{\alpha}}\right) \frac{2d}{D^2} dd \right]_{s=1},
 \end{aligned} \tag{C1}$$

where (e) follows the differentiation of definite integral [1]. Taking some algebraic manipulation proves $\mathcal{P}_{DS}^{RW}(\mathcal{R}_{th})$. Applying similar proof, we also obtain $\mathcal{P}_{RS}^{RW}(\mathcal{R}_{th})$, $\mathcal{P}_{DS}^{RWP}(\mathcal{R}_{th})$, and $\mathcal{P}_{RS}^{RWP}(\mathcal{R}_{th})$. The differentiation $\frac{\partial^n}{\partial s^n}(f(s)g(s))$ can be calculated using the Leibniz' s rule and the Faà di Bruno' s formula [1].

Appendix D System parameters for numerical simulation

Table D1 System Parameters for Numerical Simulation

Parameter	Symbol	Value
Cell Radius	D	800 m
Transmit Power of the eNodeB	P_B	29 dBm
Transmit Power of Mobile Relays	P_R	3 dBm
Number of Interfering BS Tiers	K	2
Modification Factors	η_{BW}, η_{SINR}	0.75, 1.25
Transmit Powers of Interfering BSs	P_1, P_2	13 dBm, 3 dBm
Distance between the mobile relay and the typical VUE	$d_{R,V}$	5m
Noise Power	N_0	2.3×10^{-15} W
Values of the Path Loss Exponent	α	{3,4}
Values of the Nakagami fading parameter	m_j	{1,2}

Appendix E Simulation results of the ergodic transmission success probabilities

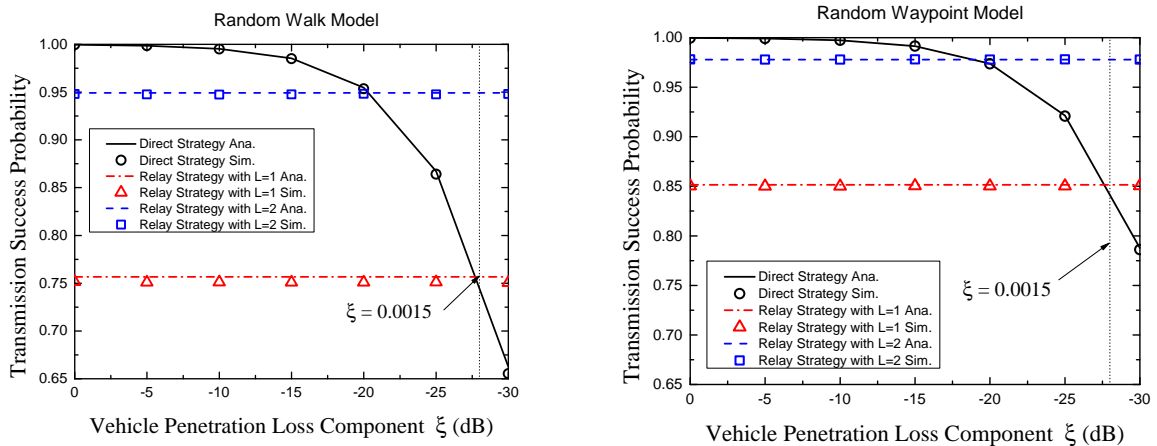


Figure E1 Transmission success probability versus VPL for the RW and RWP models in the noise-limited regime, with the Nakagami fading parameters $m_B = m_R = 1$, the path loss exponent $\alpha = 3$, and the target spectral efficiency $\mathcal{R}_{th} = 4$ bps/Hz. (a) Random walk model; (b) Random waypoint model.

In Fig. E1, we present the ergodic transmission success probabilities of the typical VUE over VPL for different numbers of antennas under the RW and RWP models in the noise-limited regime. We observe that, when the VPL (ξ^{-1}) is larger than 20dB, the *relay* strategy with two antennas can increase the ergodic transmission success probability of the typical VUE. Numerical results show that, in the noise-limited regime, the ergodic transmission success probabilities of the *relay* strategy is constrained by the transmission success probability from the eNodeB to the mobile relay. Under the considered scenario, it appears that the ergodic transmission success probability of the *relay* strategy with a single antenna in the noise-limited regime is larger than that of the *direct* strategy when $\xi \leq (2^{\mathcal{R}_{th}/\eta_{\text{BW}}} + 1)^{-1} \approx -28$ dB.

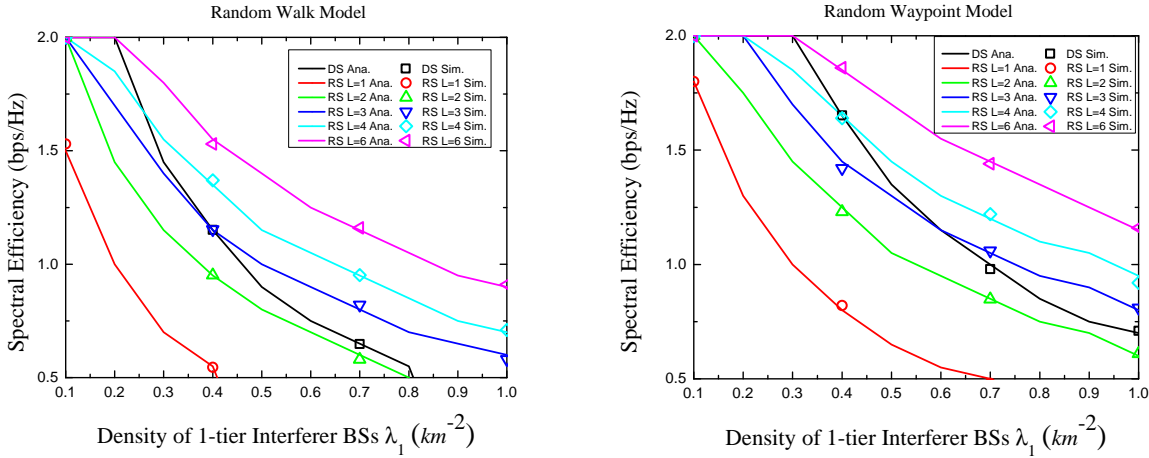


Figure E2 Capable regions in the interference-limited regime for the ergodic transmission success probability constraint $P_{j,u} \geq 0.8$, with the density of 2-tier interfering BSs $\lambda_2 = 5\lambda_1$, the Nakagami fading parameters $m_B = m_R = m_I = 2$, the path loss exponent $\alpha = 3$, and the VPL $\xi = -25$ dB. (a) Random walk model; (b) Random waypoint model.

In Fig. E2, we show the *capable regions* of different strategies in the interference-limited regime. The *capable region* is defined as the enclosure of all feasible sets of both spectral efficiency thresholds and the densities of interfering BSs for which a definite ergodic transmission success probability constraint is satisfied, shown as the area under the corresponding line. The *capable regions* can be used to evaluate the required number of antennas under different circumstances. In addition, due to the concentrated node distribution of the RWP model, the *capable region* of the RWP model is always larger than that of the RW model. Analytical results are also consistent with numerical results.

Appendix F Distance-based strategy selection algorithm

In this section, we illustrate that these analytical expressions on the transmission success probabilities of the typical VUE can be applied to design a strategy selection algorithm. We focus on the strategy selection of the *relay* or *direct* strategies, which aims to maximize the throughput of the typical VUE. Intuitively, we should allow the typical VUE to select the *relay* strategy rather than the *direct* strategy when $\mathcal{R}_{B,V} < \frac{1}{2} \min\{\mathcal{R}_{B,R}, \mathcal{R}_{R,V}\}$. Thus, we present a Spectral Efficiency based Strategy Selection (SESS) algorithm, which serves as a benchmark for performance evaluation. The SESS algorithm updates strategy selection every T ms and the strategy selection of current duration is based on the observation of previous duration. The SESS algorithm is described in Algorithm F1.

Note that the SESS algorithm induces large signaling overhead and frequent strategy switch due to the fast fading feature of Nakagami fading channels. For the practical interest of reducing the feedback overhead, we propose a Distance-based Strategy Selection (DSS) algorithm, which uses the difference between the transmission success probabilities of the *direct* and *relay* strategies as a decision parameter. Specifically, the decision function of the DSS algorithm is defined as

$$\mathcal{D}(d) = \mathbf{1}\{\mathcal{P}_{\text{DS}}(\mathcal{R}_{\text{th}}, d) - \mathcal{P}_{\text{RS}}(\mathcal{R}_{\text{th}}, d)\}, 0 < d \leq D, \quad (\text{F1})$$

where $\mathbf{1}\{x\}$ is the unit step function defined as

$$\mathbf{1}\{x\} = \begin{cases} 1 \triangleq \text{direct strategy,} & \text{for } x \geq 0, \\ 0 \triangleq \text{relay strategy,} & \text{for } x < 0. \end{cases} \quad (\text{F2})$$

In addition, when the B-V link follows the Rayleigh fading ($m_B = 1$), a simplified decision function is proposed in the following proposition for Single-Input Single-Output (SISO) scenario with $\alpha = 4$.

Algorithm F1 SE-based Strategy Selection (SESS) Algorithm

-
- 1: Let t be the index of transmission time interval (TTI). Initialize $t = 1$.
 - 2: Let \mathcal{D} denote the chosen strategy, with $\mathcal{D} = 1$ for the *direct* strategy and $\mathcal{D} = 0$ for the *relay* strategy.
 - 3: Initialize $\mathcal{D} = 1$.
 - 4: Let T denote the decision interval of the SESS algorithm.
 - 5: // Taking the typical VUE as an example
 - 6: **while** The typical VUE is active **do**
 - 7: The eNodeB communicates with the typical VUE using the chosen strategy \mathcal{D} .
 - 8: Both the typical VUE and the mobile relay estimate the channel quality indicators (CQIs) of three links based on downlink reference signal received power (RSRP).
 - 9: The typical VUE feedbacks the CQIs of both the direct and access links per TTI. The mobile relay feedbacks the CQI of the backhaul link per TTI.
 - 10: The eNodeB evaluates the spectral efficiency $\mathcal{R}_{\text{DS},t}$ and $\mathcal{R}_{\text{RS},t}$ during slot t based on previous channel estimation.
 - 11: **if** $t = nT$, where n is an integer **then**
 - 12: $\overline{\mathcal{R}}_{\text{DS}} = \sum_{t-T+1}^t \mathcal{R}_{\text{DS},t}$,
 - 13: $\overline{\mathcal{R}}_{\text{RS}} = \sum_{t-T+1}^t \mathcal{R}_{\text{RS},t}$,
 - 14: $\mathcal{D} = \mathbf{1}\{\overline{\mathcal{R}}_{\text{DS}} - \overline{\mathcal{R}}_{\text{RS}}\}$.
 - 15: **end if**
 - 16: Wait for next TTI, i.e., $t = t + 1$.
 - 17: **end while**
-

Algorithm F2 Distance-based Strategy Selection (DSS) Algorithm

-
- 1: **Require:** $L, m_{\text{B}}, m_{\text{R}}, m_{\text{I}}, P_{\text{B}}, K, P_k, \lambda_k, \rho, N_0, \xi, \alpha, \mathcal{R}_{\text{th}}$.
 - 2: Let t be the index of TTI. Initialize $t = 1$.
 - 3: Let T denote the decision interval of the DSS algorithm.
 - 4: The eNodeB collects key network parameters and calculates the transmission success probabilities of both the *direct* and *relay* strategies according to Proposition 1.
 - 5: The eNodeB calculates the decision vector according to (F1).
 - 6: The eNodeB broadcasts the decision vector to both the mobile relays and VUEs.
 - 7: // Taking the typical VUE as an example
 - 8: **while** The typical VUE is active **do**
 - 9: The typical VUE estimates and reports the distance between the eNodeB and itself at time t based on localization algorithm, e.g., Global Positioning System (GPS).
 - 10: Both the eNodeB and the typical VUE update the decision function (F1).
 - 11: The eNodeB communicates with the typical VUE using the corresponding strategy (F1).
 - 12: Wait for T milliseconds, i.e., $t = t + T$.
 - 13: **end while**
-

Proposition 1. For $L = 1$, $m_{\text{B}} = 1$, and $\alpha = 4$, the decision function (F1) can be simplified as

$$\mathcal{D}(d) = \begin{cases} 1, & \text{for } \xi\beta_{\text{B,R}} \leq \beta_{\text{B,V}} \leq \beta_{\text{B,R}} \text{ and } d \in [d^-, d^+], \\ & \text{or } \xi\beta_{\text{B,R}} > \beta_{\text{B,V}} \text{ and } d \in [d^+, \infty], \\ 0, & \text{otherwise,} \end{cases} \quad (\text{F3})$$

where d^- and d^+ , assumed $d^- < d^+$, are the solutions of the following equation

$$\left(\frac{\beta_{\text{B,V}}}{\xi} - \beta_{\text{B,R}}\right) \frac{N_0}{P_{\text{B}}} d^4 + \sum_{k=1}^K \pi\psi_k \frac{\left(\beta_{\text{B,V}}^{\frac{2}{\alpha}} - \beta_{\text{B,R}}^{\frac{2}{\alpha}}\right)}{P_{\text{B}}^{\frac{2}{\alpha}}} d^2 = \ln \mathcal{P}_{\text{R,V}}(\mathcal{R}_{\text{th}}). \quad (\text{F4})$$

Proof. Assuming $L = 1$, $m_{\text{B}} = 1$, and $\alpha = 4$, dividing $\mathcal{P}_{\text{RS}}(\mathcal{R}_{\text{th}}, d)$ with $\mathcal{P}_{\text{DS}}(\mathcal{R}_{\text{th}}, d)$ yields

$$\frac{\mathcal{P}_{\text{RS}}(\mathcal{R}_{\text{th}}, d)}{\mathcal{P}_{\text{DS}}(\mathcal{R}_{\text{th}}, d)} = \mathcal{P}_{\text{R,V}}(\mathcal{R}_{\text{th}}) \cdot \exp\left(\frac{N_0}{P_{\text{B}}}\left(\frac{\beta_{\text{B,V}}}{\xi} - \beta_{\text{B,R}}\right)d^4\right) \exp\left(\sum_{k=1}^K \pi\psi_k d^2 P_{\text{B}}^{-\frac{2}{\alpha}}\left(\beta_{\text{B,V}}^{\frac{2}{\alpha}} - \beta_{\text{B,R}}^{\frac{2}{\alpha}}\right)\right). \quad (\text{F5})$$

Let $\mathcal{P}_{\text{RS}}(\mathcal{R}_{\text{th}}, d) = \mathcal{P}_{\text{DS}}(\mathcal{R}_{\text{th}}, d)$, we have

$$\left(\frac{\beta_{\text{B,V}}}{\xi} - \beta_{\text{B,R}}\right) \frac{N_0}{P_{\text{B}}} d^4 + \sum_{k=1}^K \pi\psi_k \frac{\left(\beta_{\text{B,V}}^{\frac{2}{\alpha}} - \beta_{\text{B,R}}^{\frac{2}{\alpha}}\right)}{P_{\text{B}}^{\frac{2}{\alpha}}} d^2 = \ln \mathcal{P}_{\text{R,V}}(\mathcal{R}_{\text{th}}). \quad (\text{F6})$$

Based on the characteristics of quadratic equation, we have

$$\frac{\mathcal{P}_{\text{RS}}(\mathcal{R}_{\text{th}}, d)}{\mathcal{P}_{\text{DS}}(\mathcal{R}_{\text{th}}, d)} \begin{cases} \leq 1, & \text{for } \xi\beta_{\text{B,R}} \leq \beta_{\text{B,V}} \leq \beta_{\text{B,R}} \text{ and } d \in [d^-, d^+], \\ & \text{or } \xi\beta_{\text{B,R}} > \beta_{\text{B,V}} \text{ and } d \in [d^+, \infty], \\ > 1, & \text{Otherwise,} \end{cases} \quad (\text{F7})$$

where d^- and d^+ , assumed $d^- < d^+$, are the solutions of (F6).

Table F1 Overhead Comparison for Strategy Selection

Overhead	SESS	DSS
CSI of direct links (B ↔ V)	Y	N
CSI of backhaul links (B ↔ R)	Y	N
CSI of access links (R ↔ V)	Y	N
Location of a vehicle when $t = nT$	N	Y

Furthermore, the DSS algorithm is described in Algorithm F2. Since the decision function of the DSS algorithm can be calculated based on key network parameters, the signaling feedback required at the eNodeB is only the location of the vehicle when $t = nT$. In comparison, the overhead of signaling feedback in the SESS algorithm is considerably large, because the SESS algorithm acquires full CSI of the three links before the strategy selection. Table F1 summarizes the difference of the signaling overhead between the SESS and DSS algorithms.

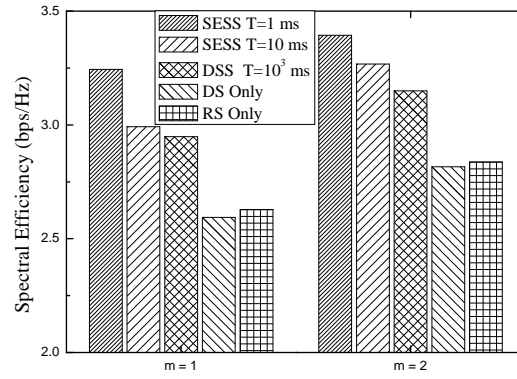


Figure F1 Spectral efficiency for the $m = 1$ and $m = 2$ cases, with $L = 1$, $\xi = -25$ dB, $\lambda_1 = 0.1 \text{ km}^{-2}$, $\lambda_2 = 0.5 \text{ km}^{-2}$, and $\mathcal{R}_{\text{th}}=1$ bps/Hz.

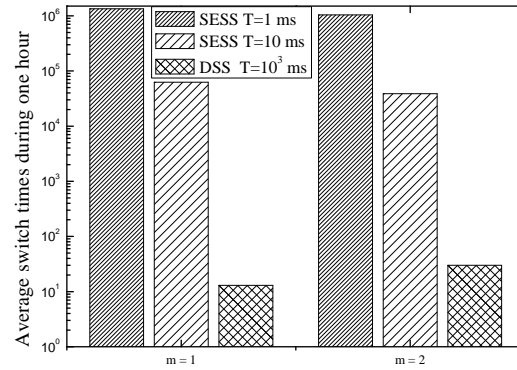


Figure F2 Average switch times for the $m = 1$ and $m = 2$ cases, with $L = 1$, $\xi = -25$ dB, $\lambda_1 = 0.1 \text{ km}^{-2}$, $\lambda_2 = 0.5 \text{ km}^{-2}$, and $\mathcal{R}_{\text{th}}=1$ bps/Hz.

In Fig. F1, we show the numerical results on the spectral efficiency in $m = 1$ and $m = 2$ cases. The SESS algorithm with $T = 1$ ms has the highest spectral efficiency, while the DSS algorithm with $T = 10^3$ ms achieves considerably high spectral efficiency compared with either the *direct* strategy (DS Only) or the *relay* Strategy (RS Only). Specifically, in the

$m = 1$ case, the performance loss of the DSS algorithm with $T = 10^3$ ms is 0.29 and 0.04 bps/Hz compared with the SESS algorithm with $T = 1$ ms and $T = 10$ ms, respectively. And the performance gain of the DSS algorithm with $T = 10^3$ ms is 0.35 and 0.32 bps/Hz compared with the DS Only and RS Only algorithms, respectively. In the $m = 2$ case, the performance loss of the DSS algorithm with $T = 10^3$ ms is 0.24 and 0.12 bps/Hz compared with the SESS algorithm with $T = 1$ ms and $T = 10$ ms, respectively. And the performance gain of the DSS algorithm with $T = 10^3$ ms is 0.33 and 0.31 bps/Hz compared with the DS Only and RS Only algorithms, respectively.

In Fig. F2, we present the average switch times of the SESS algorithm with $T = 1, 10$ ms and the DSS algorithm with $T = 10^3$ ms during one hour. We see that average switch times of the SESS algorithm with $T = 1, 10$ ms and the DSS algorithm with $T = 10^3$ ms are $O(10^6)$, $O(10^5)$, and $O(10)$, respectively. Therefore, although the DSS algorithm has some performance loss compared with the SESS algorithm, the fluctuation of the DSS algorithm in terms of strategy switch is substantially smaller than that of the SESS algorithm.

References

- 1 Daniel Zwillinger. Table of integrals, series, and products. Elsevier, 2014.
- 2 Ralph Tanbourgi, Harpreet S. Dhillon, Jeffrey G. Andrews, et al. Dual-branch MRC receivers under spatial interference correlation and Nakagami fading. *IEEE Trans. Commun.*, 2014, 62(6):1830-1844.
- 3 Martin Haenggi and Radha Krishna Ganti. Interference in large wireless networks. Now Publishers Inc, 2009.